*Article*

# Simplified Two-Dimensional Generalized Partial Response Target of Holographic Data Storage Channel

Thien An Nguyen [ID] and Jaejin Lee *[ID]

Department of Information Communication Convergence Technology, Soongsil University, Seoul 06978, Korea; anthienng1995@soongsil.ac.kr
* Correspondence: zlee@ssu.ac.kr; Tel.: +82-2-820-0901

**Abstract:** With a high capacity and fast data access rate, holographic data storage (HDS) is a potential candidate for future storage systems. However, for page-oriented data processing, two-dimensional (2D) interference appears intensely in the HDS systems. Therefore, the new 2D generalized partial response (GPR) target is introduced to estimate the 2D interference. In addition, we also propose a method to analyze the 2D GPR target into two serial one-dimensional (1D) GPR targets. It makes us design a simple detection scheme composed of two serial 1D detectors instead of a complicated 2D detector. In simulations, the results show that our proposed scheme can improve the BER performance compared to the conventional 1D GPR target model.

**Keywords:** holographic data storage; estimating interference; remove interference; detection; decomposing interference

## 1. Introduction

Due to the demand for storage increasing at a high rate, devices with high capacity and fast transfer are a matter of common interest. At present, semiconductor memories [1] and magnetic hard disk drives [2] are widely used in many devices. However, unlike semiconductor memories and magnetic hard disk drives, holographic data storage systems can read out 2D data page bits at the same time [3]. Therefore, holographic data storage achieves a high data transfer rate. In addition, many researchers have proposed methods to multiplex multiple pages of data by changing the angle [4], wavelength [5,6], or phase code [7,8] of the reference beam. This helps to improve the capacity of the HDS and meet the requirements of greater capacity and fast transfer [3,9].

Therefore, the holographic data storage (HDS) system is a promising candidate for mass-storage devices. In HDS systems, the data are converted into the beam and stored on the holographic medium. Then, to read back the data, we use the reference beam to reconstruct the beam from the holographic medium. The image of the data is captured by a charge-coupled device (CCD). The data page suffers from blurring effects; therefore, the read-back data always face two serious problems. One is inter-page interference (IPI) between the pages, and another is two-dimensional (2D) inter-symbol interference (ISI) that appears on the data page of the HDS systems. To avoid IPI, the numbers of one and zero pixels must be almost equal on each page [10]. To implement this, we can use balanced coding, which ensures the intensity level of each page is the same [11]. Among these factors, 2D ISI is regarded as the main causative reason. To combat ISI, based on the one-dimensional (1D) partial response maximum likelihood (PRML) detection scheme in [12], Kim and Lee proposed the 2D soft-output Viterbi algorithm (SOVA) as the 2D detection for the HDS systems [13]. Then, the 2D SOVA is improved and applied to the bit-patterned media recording (BPMR) channel [14,15]. In 2D SOVA, the authors use two parallel 1D PRML to remove the 1D interference from the horizontal and vertical directions. In addition, Nabavi and Kumar [16] propose a general partial response (GPR) target, which achieves better performance than PRML. Then, the GPR target is developed and utilized

in [17–22]. However, the authors only estimate 1D interference (i.e., designing a 1D GPR target) to avoid the 2D detection in [16]. In [22], to handle 2D interference, the authors introduce the estimator interference with a parallel structure to convert 2D interference into 1D interference. Although achieving high performance, the model in [22] has high complexity. In [23], the authors propose the decision feedback equalizer (DFE) to recover the original from the received signal, which is distorted by the 2D ISI. The DFE model is a simple method to solve 2D ISI, but the performance of the DFE model is unsatisfactory because of the simple detection scheme. Therefore, in this paper, we improve the GPR target for 2D interference. From the estimated 2D GPR target, we propose a simple method to decompose 2D ISI into two serial 1D vertical direction ISI and 1D horizontal direction ISI. From here, we can use the serial detection [21] to recover the original data from the HDS systems. In simulation, the result shows that our proposed model achieves a gain of 2.5 dB at the BER $10^{-3}$ compared to the 1D GPR target in [16].

In the remainder of this paper, we explain the 2D GPR target and serial detection in Section 2. In Section 3, we present the proposed model. Section 4 presents and discusses the simulations and results. Finally, in Section 5, the conclusions are drawn.

## 2. 2D GPR Target and Serial Detection

### 2.1. 2D GPR Target

First, we estimate the coefficients of the 2D GPR target and 2D equalizer in the training process. The model for the training process is presented in Figure 1.
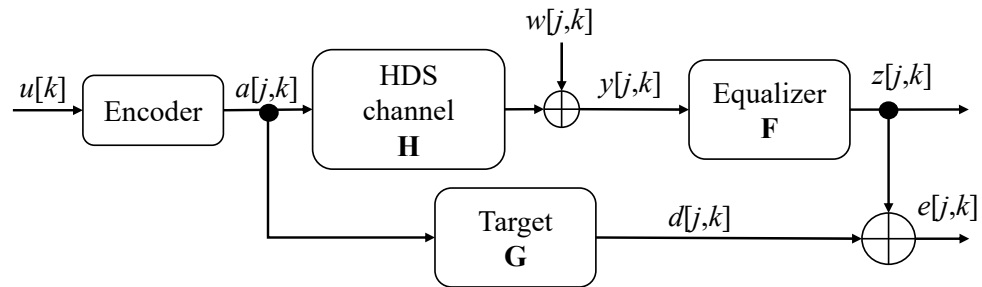


**Figure 1.** Training process model.

To design and implement the 2D GPR target and equalizer, we use the GPR target **G** with a size of $3 \times 3$, and the equalizer **F** with a size of $5 \times 5$; these are presented as in the below matrices.

$$\mathbf{G} = \begin{bmatrix} g_{-1,-1} & g_{-1,0} & g_{-1,1} \\ g_{0,-1} & g_{0,0} & g_{0,1} \\ g_{1,-1} & g_{1,0} & g_{1,1} \end{bmatrix}, \tag{1}$$

$$\mathbf{F} = \begin{bmatrix} f_{-2,-2} & f_{-2,-1} & f_{-2,0} & f_{-2,1} & f_{-2,2} \\ f_{-1,-2} & f_{-1,-1} & f_{-1,0} & f_{-1,1} & f_{-1,2} \\ f_{0,-2} & f_{0,-1} & f_{0,0} & f_{0,1} & f_{0,2} \\ f_{1,-2} & f_{1,-1} & f_{1,0} & f_{1,1} & f_{1,2} \\ f_{2,-2} & f_{2,-1} & f_{2,0} & f_{2,1} & f_{2,2} \end{bmatrix}. \tag{2}$$

With matrices **G** and **F**, we can achieve the signals $d[j,k]$ and $z[j,k]$, as follows:

$$d[j,k] = \sum_{m=-1}^{1} \sum_{n=-1}^{1} a[j-m, k-n] g_{m,n}$$

$$= \begin{bmatrix} a[j+1, k+1] & \dots & a[j,k] & \dots & a[j-1, k-1] \end{bmatrix} \begin{bmatrix} g_{-1,-1} \\ g_{-1,0} \\ \vdots \\ g_{1,1} \end{bmatrix} \tag{3}$$

$$z[j,k] = \sum_{m=-2}^{2} \sum_{n=-2}^{2} y[j-m,k-n] f_{m,n}$$

$$= \begin{bmatrix} y[j+2,k+2] & \cdots & y[j,k] & \cdots & a[j-2,k-2] \end{bmatrix} \begin{bmatrix} f_{-2,-2} \\ f_{-2,-1} \\ \vdots \\ f_{2,2} \end{bmatrix} \tag{4}$$

We assign the vectors as follows:

$$\mathbf{a} = \begin{bmatrix} a[j+1,k+1] & \cdots & a[j-1,k-1] \end{bmatrix}^T, \tag{5}$$

$$\mathbf{g} = \begin{bmatrix} g_{-1,-1} & g_{-1,0} & \cdots & g_{1,1} \end{bmatrix}^T, \tag{6}$$

$$\mathbf{y} = \begin{bmatrix} y[j+2,k+2] & \cdots & y[j-2,k-2] \end{bmatrix}^T, \text{ and} \tag{7}$$

$$\mathbf{f} = \begin{bmatrix} f_{-2,-2} & f_{-2,-1} & \cdots & f_{2,2} \end{bmatrix}^T. \tag{8}$$

Using the definitions from (5) to (8), we can rewrite (3) and (4) as follows:

$$d[j,k] = \mathbf{g}^T \mathbf{a}, \tag{9}$$

$$z[j,k] = \mathbf{f}^T \mathbf{y}. \tag{10}$$

We find **g** and **f** in order that $z[j,k]$ is close to $d[j,k]$. To implement this, we apply the minimum mean square error (MMSE) algorithm. This problem is presented as follows:

$$\underset{\mathbf{f},\mathbf{g}}{\operatorname{argmin}} E\left\{ (z[j,k] - d[j,k])^2 \right\} = \underset{\mathbf{f},\mathbf{g}}{\operatorname{argmin}} E\left\{ \left( \mathbf{g}^T \mathbf{a} - \mathbf{f}^T \mathbf{y} \right)^2 \right\}, \tag{11}$$

where $E$ denotes the expectation. We can expand (11) as follows:

$$\underset{\mathbf{f},\mathbf{g}}{\operatorname{argmin}} \left( \mathbf{f}^T E\left\{ \mathbf{y}\mathbf{y}^T \right\} \mathbf{f} - 2\mathbf{f}^T E\left\{ \mathbf{y}\mathbf{a}^T \right\} \mathbf{g} + \mathbf{g}^T E\left\{ \mathbf{a}\mathbf{a}^T \right\} \mathbf{g} \right) \tag{12}$$

Since the trivial answer for minimizing (12) is **f** = **g** = 0, we must impose the constraint on **f** or **g**. The constraint is represented by the below expression.

$$\mathbf{E}^T \mathbf{g} = c, \tag{13}$$

where $c$ is an estimated multiplier of the center data and investigated in Section 4, and

$$\mathbf{E}^T = \begin{bmatrix} 0 & 0 & 0 & 0 & 1 & 0 & 0 & 0 & 0 \end{bmatrix}. \tag{14}$$

With the above constraints, we can rewrite the optimal problem (12) as follows:

$$\underset{\mathbf{f},\mathbf{g}}{\operatorname{argmin}} \left( \mathbf{f}^T E\{\mathbf{y}\mathbf{y}^T\} \mathbf{f} - 2\mathbf{f}^T E\{\mathbf{y}\mathbf{a}^T\} \mathbf{g} + \mathbf{g}^T E\{\mathbf{a}\mathbf{a}^T\} \mathbf{g} \right)$$
$$\text{s.t. } \mathbf{E}^T \mathbf{g} = c \tag{15}$$

To solve (15), we use the Lagrange function, as follows:

$$J = \mathbf{f}^T E\left\{ \mathbf{y}\mathbf{y}^T \right\} \mathbf{f} - 2\mathbf{f}^T E\left\{ \mathbf{y}\mathbf{a}^T \right\} \mathbf{g} + \mathbf{g}^T E\left\{ \mathbf{a}\mathbf{a}^T \right\} \mathbf{g} - 2\lambda \left( \mathbf{E}^T \mathbf{g} - c \right). \tag{16}$$

where $\lambda$ is a vector containing the Lagrange multipliers. By setting the gradients of $J$ with respect to **f**, **g**, and $\lambda$ to zero vectors, we achieve the answers to (15) as follows:

$$\lambda = \left( \mathbf{E}^T \left( \mathbf{A} - \mathbf{T}^T \mathbf{R}^{-1} \mathbf{T} \right)^{-1} \mathbf{E} \right)^{-1} c, \tag{17}$$

$$\mathbf{g} = \left( \mathbf{A} - \mathbf{T}^T \mathbf{R}^{-1} \mathbf{T} \right)^{-1} \mathbf{E}\lambda, \text{ and} \tag{18}$$

$$\mathbf{f} = \mathbf{R}^{-1} \mathbf{T} \mathbf{g}. \tag{19}$$

where $\mathbf{A} = E\{\mathbf{a}\mathbf{a}^T\}$, $\mathbf{R} = E\{\mathbf{y}\mathbf{y}^T\}$, and $\mathbf{T} = E\{\mathbf{y}\mathbf{a}^T\}$.

### 2.2. Proposed Serial Detection

After the coefficients of the GPR target are estimated by the MMSE algorithm, the GPR target has a matrix form like (1). In the HDS channel, the read-back signal is the Gaussian beam. Therefore, the interference coefficients from the adjacent pixels can be given by the values from the Gaussian function. Based on these coefficients, we assume the conditions: $g_{-1,0} = g_{1,0} = g_{0,1} = g_{0,-1}$ and $g_{-1,-1} = g_{-1,1} = g_{1,-1} = g_{1,1}$. Then, we can decompose $\mathbf{G}$ as given below.

$$\mathbf{G} = \begin{bmatrix} g_{-1,-1} & g_{-1,0} & g_{-1,1} \\ g_{0,-1} & g_{0,0} & g_{0,1} \\ g_{1,-1} & g_{1,0} & g_{1,1} \end{bmatrix} = \begin{bmatrix} p \\ l_1 \\ p \end{bmatrix} \begin{bmatrix} r & l_2 & r \end{bmatrix}. \tag{20}$$

where $r$ and $p$ are the horizontal and vertical interferences, respectively; $l_1$ and $l_2$ are the general parameters to fit the form of the GPR target $\mathbf{G}$. In other words, the 2D GPR target $\mathbf{G}$ with 2D ISI is decomposed into a series of 1D vertical direction interference vector $\mathbf{v} = [p\ l_1\ p]^T$ and 1D horizontal direction interference vector $\mathbf{b} = [r\ l_2\ r]$. Then, $\mathbf{v}$ and $\mathbf{b}$ act like the outer and inner encoders, respectively. Therefore, we detect the horizontal direction first and the vertical direction next. The serial detection of the ideal channel model is illustrated in Figure 2.
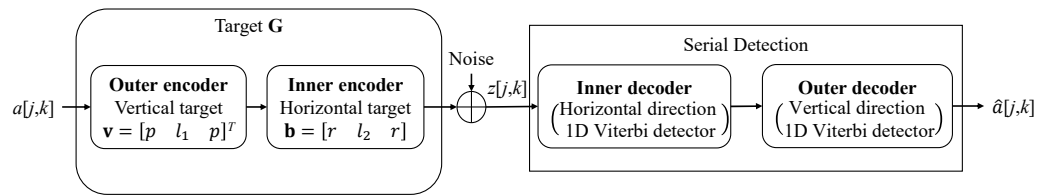


**Figure 2.** Ideal channel and detection model.

With the proposed form $\mathbf{v}$ and $\mathbf{b}$, we achieve the following expression:

$$\mathbf{G} = \begin{bmatrix} rp & l_2 p & rp \\ rl_1 & l_1 l_2 & rl_1 \\ rp & l_2 p & rp \end{bmatrix}, \tag{21}$$

Since $(l_2 p)(rl_1) = (l_1 l_2)(rp)$, the parameters of the matrix $\mathbf{G}$ must satisfy the condition $g_{0,0}g_{-1,1} = g_{-1,0}g_{0,1}$. When we implement the estimation of the GPR target for the HDS channel, the coefficients of the GPR target shows $g_{0,0}g_{-1,1} \approx g_{-1,0}g_{0,1}$, which is close to the above condition. Therefore, we can match the parameters between the GPR target $\mathbf{G}$ and the matrix $\mathbf{v}\mathbf{b}$ to determine the elements of the vector $\mathbf{v}$ and $\mathbf{b}$. To simplify, we choose the parameter $l_1 = 1$ and determine other parameters with the formulas:

$$r = g_{0,1}, \tag{22}$$

$$p = \frac{g_{1,0}}{g_{0,0}}, \tag{23}$$

$$l_2 = g_{0,0}. \tag{24}$$

With the parameters $r$, $p$, $l_1$, and $l_2$, we can achieve the vector $\mathbf{v}$ and $\mathbf{b}$. Therefore, we can apply two 1D Viterbi detectors for the serial detection [18,20,21] with the interference coefficient supplied from the target vector $\mathbf{v}$ and $\mathbf{b}$ to recover the original data.

In addition, when misalignment occurs in the HDS channel, the vectors **v** and **b** have the asymmetric form as below.

$$\mathbf{G} = \begin{bmatrix} g_{-1,-1} & g_{-1,0} & g_{-1,1} \\ g_{0,-1} & g_{0,0} & g_{0,1} \\ g_{1,-1} & g_{1,0} & g_{1,1} \end{bmatrix} = \begin{bmatrix} p_1 \\ l_1 \\ p_2 \end{bmatrix} \begin{bmatrix} r_1 & l_2 & r_2 \end{bmatrix} = \begin{bmatrix} r_1 p_1 & l_2 p_1 & r_2 p_1 \\ r_1 l_1 & l_1 l_2 & r_2 l_1 \\ r_1 p_2 & l_2 p_2 & r_2 p_2 \end{bmatrix}. \tag{25}$$

Similarly, we can achieve the approximated parameters as below.

$$l_1 = 1; l_2 = g_{0,0}, \tag{26}$$

$$r_1 = g_{0,-1}; r_2 = g_{0,1}, \tag{27}$$

$$p_1 = \frac{g_{-1,0}}{l_2}; p_2 = \frac{g_{1,0}}{l_2}. \tag{28}$$

## 3. Proposed Model

Figure 3 shows the simulation model of the proposed scheme exploiting two 1D Viterbi detections based on the two target vectors **v** and **b**.
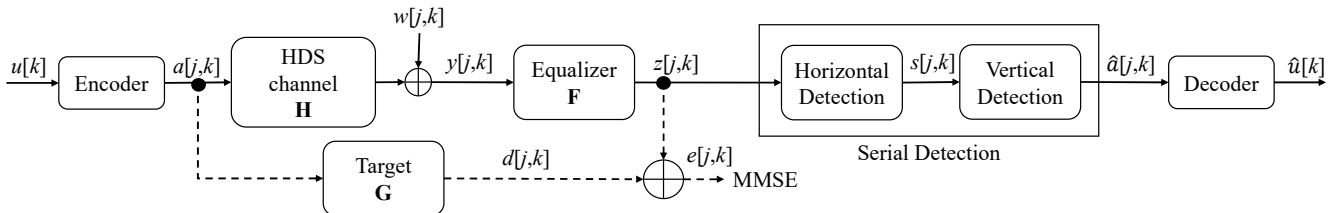


**Figure 3.** Proposed simulation model.

In this model, using a spatial light modulator (SLM), the original data $u[k]$ are encoded into the data $a[j,k]$ and stored on the holographic medium. To read back the data, we apply the reference beam onto the holographic medium. The data page is displayed and read by a CCD [23]. Then, the read-back signal suffers from blurring effects (2D ISI), additive noise, and misalignment. Thus, the signal $y[j,k]$ is presented as follows [23–25]:

$$y[j,k] = a[j,k] \otimes h[j,k] + w[j,k], \tag{29}$$

where $[j,k]$ is the position on the data page, $w[j,k]$ is the additive Gaussian noise with zero mean and variance $\sigma^2$, and the discrete point spread function (PSF) $h[j,k]$ is given by:

$$h[j,k] = \int_{j-1/2}^{j+1/2} \int_{k-1/2}^{k+1/2} h(x,y)dxdy. \tag{30}$$

The continuous PSF is modeled by:

$$h(x,y) = \frac{1}{\sigma_b^2}\sin c^2\left(\frac{x-m_x}{\sigma_b}, \frac{y-m_y}{\sigma_b}\right), \tag{31}$$

where $\text{sinc}(x,y) = (\sin(\pi x)/\pi x)(\sin(\pi y)/\pi y)$, $\sigma_b$ is the grade of blur in the resultant diffracted signals, and $m_x$ and $m_y$ are $x$ and $y$ axis misalignments, respectively.

Then, the read-back signal $y[j,k]$ goes through the 2D equalizer, which is updated by the MMSE algorithm. The output of the equalizer $z[j,k]$ is close to the desired signal from the GPR target (i.e., $z[j,k] \approx d[j,k] = a[j,k] \otimes \mathbf{G}$). With the GPR target estimated earlier, the signal $z[j,k]$ is detected by the serial detection and restored into the signal $\hat{a}[j,k]$. Finally, the signal $\hat{a}[j,k]$ is decoded into the original signal $\hat{u}[k]$.

## 4. Simulation Results

### 4.1. Results of Proposed Model

For the training process, the original data $u[k]$ are randomly created with the size of 1,440,000 and the same probabilities for 0 and 1. Then, $u[k]$ is encoded into a page-data $a[j,k]$ with a size of $1200 \times 1200$. The signal $a[j,k]$ and the read-back signal $y[j,k]$ are collected and used to estimate the coefficients of the GPR target and equalizer with the MMSE algorithm in Section 2. Then, these coefficients are used for the testing process. In the testing process, the coefficients from the GPR target are supplied to the serial detection in [13]. Simultaneously, we created 10 pages to evaluate the bit error rate (BER) performance of the system. In the first experiment, we investigate the constant $c$ in (13). The results are presented in Figure 4. During this experiment, we fixed the blur at 1.8, SNR = 16 dB, and 0% misalignment.
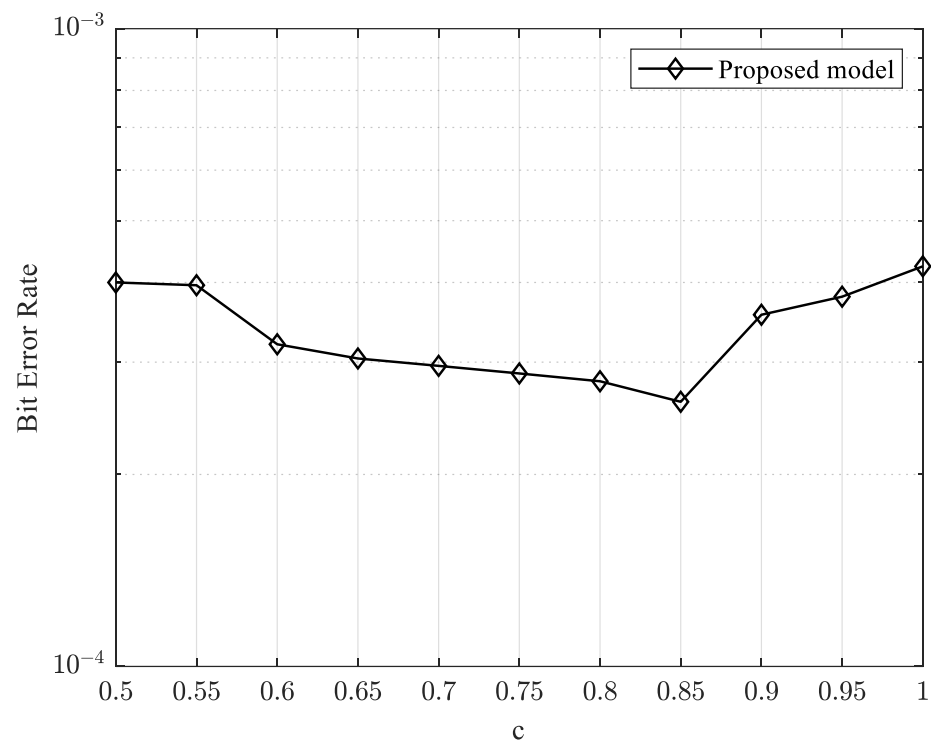


**Figure 4.** BER vs. the values of $c$.

With the results from Figure 4, we chose $c = 0.85$ and achieved the parameters of vectors **v** and **b** as in Tables 1 and 2.

**Table 1.** Parameters of the target **v** and **b** with 1.8 blur and 0% misalignment.

| SNR | G | | | v | b | | |
|---|---|---|---|---|---|---|---|
| 10 dB | 0.2 | 0.4 | 0.2 | 0.4709 | | | |
| | 0.4 | 0.85 | 0.4 | 1 | 0.4023 | 0.85 | 0.4023 |
| | 0.2 | 0.4 | 0.2 | 0.4709 | | | |
| 11 dB | 0.199 | 0.4 | 0.199 | 0.4743 | | | |
| | 0.4 | 0.85 | 0.4 | 1 | 0.4047 | 0.85 | 0.4047 |
| | 0.199 | 0.4 | 0.199 | 0.4743 | | | |
| 12 dB | 0.196 | 0.4 | 0.196 | 0.4744 | | | |
| | 0.4 | 0.85 | 0.4 | 1 | 0.4053 | 0.85 | 0.4053 |
| | 0.196 | 0.4 | 0.196 | 0.4744 | | | |

**Table 2.** Parameters of the target **v** and **b** with 1.8 blur and 10% misalignment.

| SNR | G | | | v | b | | |
|---|---|---|---|---|---|---|---|
| 10 dB | $\begin{bmatrix} 0.21 & 0.41 & 0.2 \\ 0.41 & 0.85 & 0.4 \\ 0.2 & 0.4 & 0.199 \end{bmatrix}$ | | | $\begin{bmatrix} 0.4877 \\ 1 \\ 0.4732 \end{bmatrix}$ | $\begin{bmatrix} 0.41 & 0.85 & 0.4 \end{bmatrix}$ | | |
| 11 dB | $\begin{bmatrix} 0.214 & 0.417 & 0.2 \\ 0.417 & 0.85 & 0.4 \\ 0.2 & 0.4 & 0.197 \end{bmatrix}$ | | | $\begin{bmatrix} 0.4905 \\ 1 \\ 0.4705 \end{bmatrix}$ | $\begin{bmatrix} 0.417 & 0.85 & 0.4 \end{bmatrix}$ | | |
| 12 dB | $\begin{bmatrix} 0.212 & 0.4189 & 0.2038 \\ 0.4189 & 0.85 & 0.4045 \\ 0.2038 & 0.4045 & 0.1925 \end{bmatrix}$ | | | $\begin{bmatrix} 0.4928 \\ 1 \\ 0.4758 \end{bmatrix}$ | $\begin{bmatrix} 0.4189 & 0.85 & 0.4045 \end{bmatrix}$ | | |

Next, we compared our proposed model with the 1D GPR target in [16] and the 2D SOVA in [13]. The BER performances are presented in Figures 5 and 6.
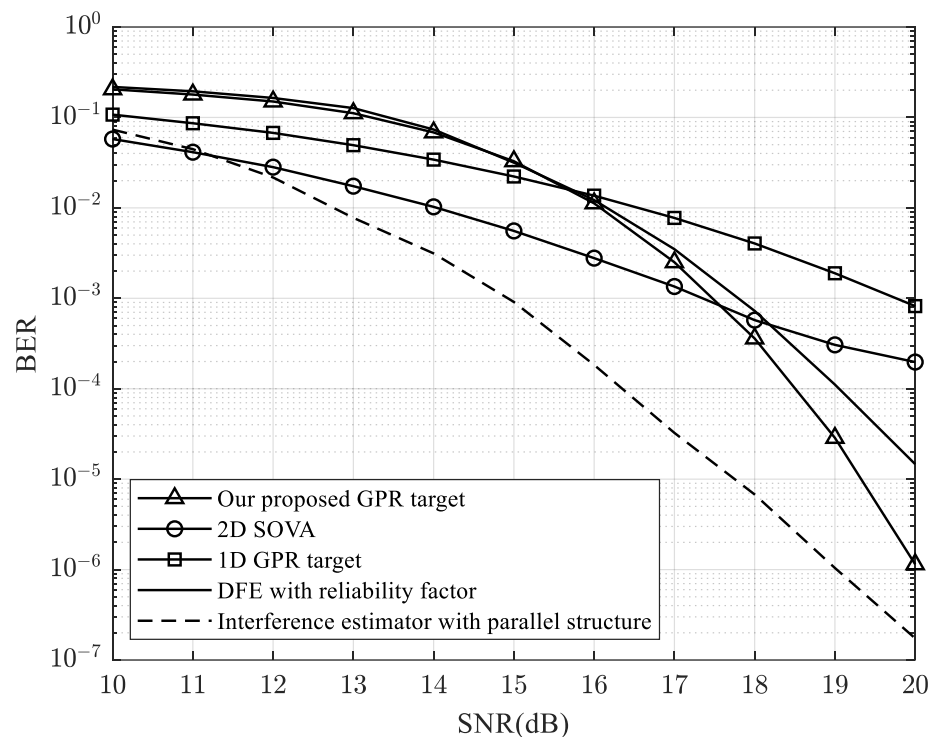


**Figure 5.** BER of the proposed 2D GPR target at 1.8 blur and 0% misalignment.

In Figures 5 and 6, the 1D GPR target model in [16] achieves similar BER performance at 0% and 10% misalignment, while the BER performance of the 2D SOVA model in [13] is significantly degraded at 10% misalignment. However, the proposed model performs almost the same, with 10% misalignment. These results show that the 2D GPR target can estimate the interference of the channel even if the misalignment effect appears. The 1D GPR target model in [13] used the partial response (PR) target, which has the fixed parameter of the target. Thus, when the misalignment appears, it cannot estimate the interference appropriately compared to the 2D GPR target. In addition, the proposed model is also compared to the DFE with reliability factor in [23], and the interference estimator with parallel structure in [22]. The interference estimator with parallel structure scheme achieves better BER performance compared to the proposed model because it is designed with the SOVA algorithm, which requires more complexity, instead of the simple VA used in the proposed model. Therefore, the proposed model can give a margin to the system designer for selecting a simple detection architecture. (Section 4.2 compares the complexity of various detection schemes.)
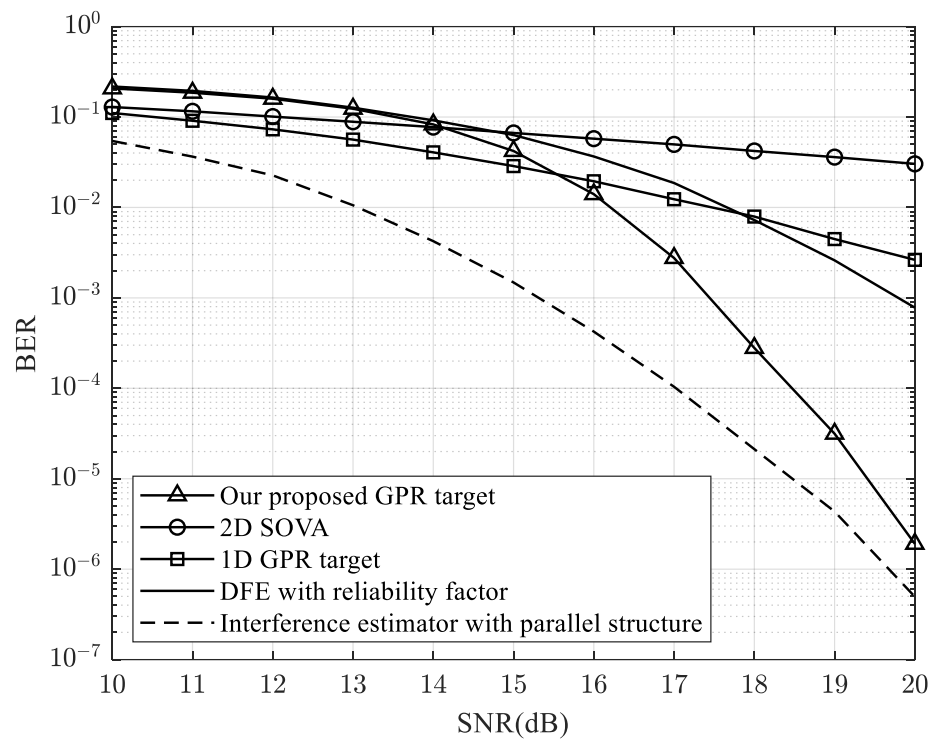
**Figure 6.** BER of the proposed 2D GPR target at 1.8 blur and 10% misalignment.

In the next experiment, to investigate the effect of the blur, we changed the blur from 1.8 to 3 with SNR = 20 dB and the results are shown in Figures 7 and 8. The proposed 2D GPR target model performs well compared to other methods.
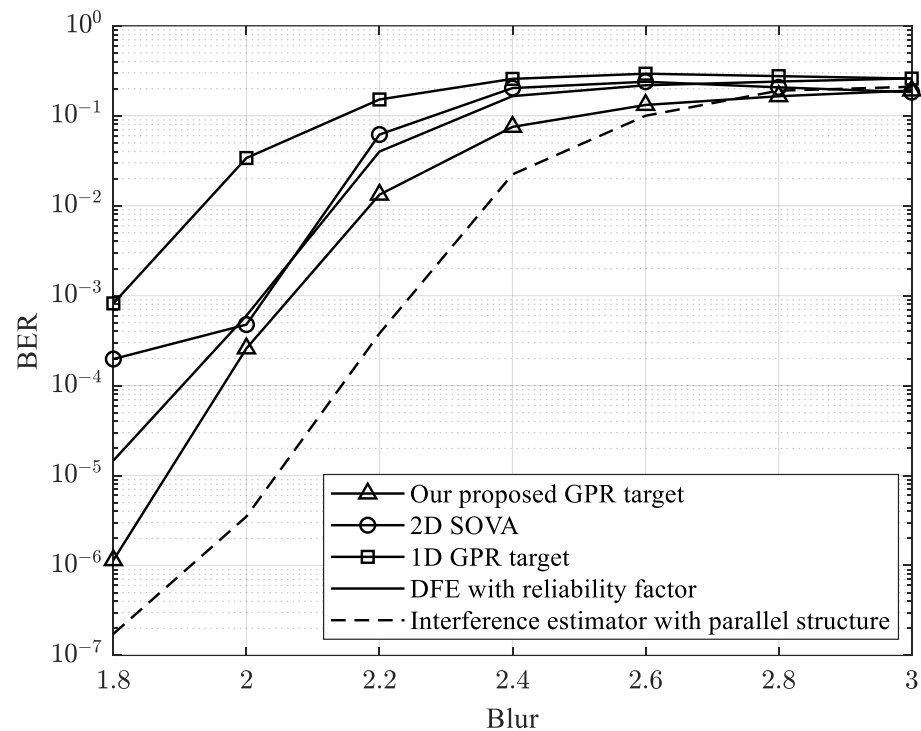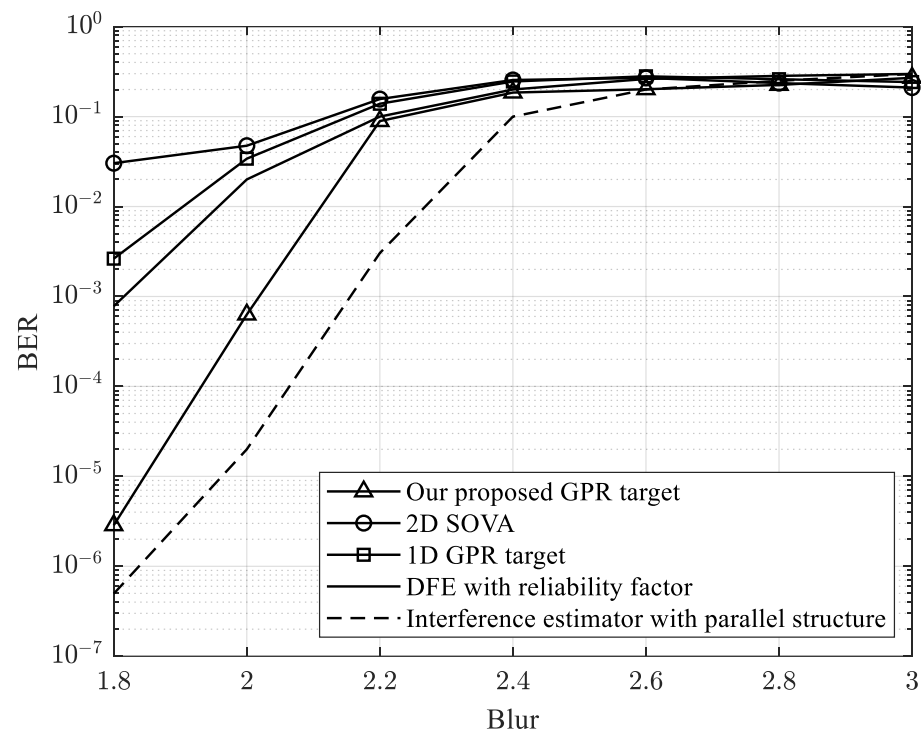


**Figure 7.** BER of the proposed GPR target varying the blur from 1.8 to 3 at 0% misalignment.

**Figure 8.** BER of the proposed GPR target varying the blur from 1.8 to 3 at 10% misalignment.

*4.2. Complexity of Proposed Model*

In this section, we compare the complexity of the proposed model, the methods in [13,16,22,23], and the complicated 2D Viterbi detector. We count the operators per the detected bit from the equalizer to the detection in each method and list them in Table 3.

**Table 3.** The complexity of the proposed and other methods.

| Methods | Mul/Div | Add/Sub |
|---|---|---|
| Our model | 252 | 700 |
| 2D SOVA [13] | 123 | 94 |
| 1D GPR [16] | 33 | 48 |
| Model in [22] | 571 | 1229 |
| DFE [23] | >36 | >34 |
| Complicated 2D Viterbi | >537 | >1560 |

In Table 3, the number of operations of the DFE model are counted for one iteration. Thus, to achieve the steady state in [23], the number of operations is larger than the numbers in Table 3. In addition, we used the general GPR target in (1) to estimate the operations for the complicated 2D Viterbi. For the GPR target in (1), the trellis of the detector has 64 states and eight input branches in each state. The proposed model takes more calculations compared to the model in [13,16]. However, our proposed model requires fewer calculations compared to the complicated 2D Viterbi and the interference estimator with parallel structure schemes.

**5. Conclusions**

In this paper, we proposed a method to decompose the 2D ISI GPR target into two serial 1D vertical and horizontal targets. Firstly, we used the general 2D GPR target to estimate the 2D interference from the HDS channel. Then, based on these interferences, we approximated the general 2D GPR target to two serial 1D targets, which includes horizontal and vertical interferences. Therefore, we can exploit the serial detection with two 1D Viterbi detectors for the HDS systems. This makes the detector very simple compared with

the complicated 2D Viterbi detector and significantly improves the performance of the HDS system.

The proposed 2D GPR target achieves similar BER performance at 0% and 10% misalignment, which means that the proposed 2D GPR target can resist the misalignment effect. The proposed 2D GPR target can provide gains of approximately 2.5 dB at $10^{-3}$ compared to the 1D GPR target [16] with 1.8 blur and 0% and 10% misalignments. In addition, our proposed method can still achieve the best performance when the blur increases.

## References

1.  Asai, S. Semiconductor memory trends. *Proc. IEEE* **1986**, *74*, 1623–1635. [CrossRef]
2.  Miura, Y. Hard disk drive technology: Past, present and future. In Proceedings of the Digest of the Asia-Pacific Magnetic Recording Conference 2002, Singapore, 27–29 August 2002.
3.  Hesselink, L.; Orlov, S.S.; Bashaw, M.C. Holographic data storage systems. *Proc. IEEE* **2004**, *92*, 1231–1280. [CrossRef]
4.  Burr, G.W.; Mok, F.H.; Psaltis, D. Angle and space multiplexed holographic storage using the 90° geometry. *Opt. Commun.* **1995**, *117*, 49–55. [CrossRef]
5.  Yu, F.T.; Wu, S.; Mayers, A.W.; Rajan, S. Wavelength multiplexed reflection matched spatial filters using $LiNbO_3$. *Opt. Commun.* **1991**, *81*, 343–347. [CrossRef]
6.  Rakuljic, G.A.; Leyva, V.; Yariv, A.; Yeh, P.; Gu, C. Optical data storage by using orthogonal wavelength-multiplexed volume holograms. *Opt. Lett.* **1992**, *17*, 1471–1473. [CrossRef]
7.  Krile, T.F.; Hagler, M.O.; Redus, W.D.; Walkup, J.F. Multiplex holography with chirp-modulated binary phase-coded refer-ence-beam masks. *Appl. Opt.* **1979**, *18*, 52–56. [CrossRef]
8.  Ford, J.E.; Fainman, Y.; Lee, S.H. Array interconnection by phase-coded optical correlation. *Opt. Lett.* **1990**, *15*, 1088–1090. [CrossRef]
9.  Vadde, V.; Kumar, B.V.K.V. Channel modeling and estimation for intrapage equalization in pixel-matched volume holo-graphic data storage. *Appl. Opt.* **1999**, *38*, 4374–4386. [CrossRef]
10. Kim, J.; Lee, J. Two-Dimensional 5:8 Modulation Code for Holographic Data Storage. *Jpn. J. Appl. Phys.* **2009**, *48*, 03A031. [CrossRef]
11. Wilson, W.Y.H.; Immink, K.A.S.; Xi, X.B.; Chong, T.C. Efficient coding technique for holographic storage using the method of guided scrambling. *Proc. SPIE* **2000**, *4090*, 191–196.
12. Cideciyan, R.; Dolivo, F.; Hermann, R.; Hirt, W.; Schott, W. A PRML system for digital magnetic recording. *IEEE J. Sel. Areas Commun.* **1992**, *10*, 38–56. [CrossRef]
13. Kim, J.; Lee, J. Two-Dimensional SOVA and LDPC Codes for Holographic Data Storage System. *IEEE Trans. Magn.* **2009**, *45*, 2260–2263. [CrossRef]
14. Kim, J.; Lee, J. Iterative Two-Dimensional Soft Output Viterbi Algorithm for Patterned Media. *IEEE Trans. Magn.* **2011**, *47*, 594–597. [CrossRef]
15. Jeong, S.; Lee, J. Iterative decoding of SOVA and LDPC product code for bit-patterned media recoding. *AIP Adv.* **2018**, *8*, 056503. [CrossRef]
16. Nabavi, S.; Kumar, B.V.K.V. Two-dimensional generalized partial response equalizer for bit-patterned media. In Proceedings of the IEEE International Conference on Communications, Glasgow, UK, 24–28 June 2007; pp. 6249–6254. [CrossRef]
17. Wang, Y.; Kumar, B.V.K.V. Improved Multitrack Detection With Hybrid 2-D Equalizer and Modified Viterbi Detector. *IEEE Trans. Magn.* **2017**, *53*, 1–10. [CrossRef]
18. Nguyen, T.A.; Lee, J. One-Dimensional Serial Detection Using New Two-Dimensional Partial Response Target Modeling for Bit-Patterned Media Recording. *IEEE Magn. Lett.* **2020**, *11*, 1–5. [CrossRef]

19.　Nguyen, T.A.; Lee, J. Modified Viterbi Algorithm with Feedback Using a Two-Dimensional 3-Way Generalized Partial Response Target for Bit-Patterned Media Recording Systems. *Appl. Sci.* **2021**, *11*, 728. [CrossRef]

20.　Nguyen, T.; Lee, J. Serial Detection with Neural Network-Based Noise Prediction for Bit-Patterned Media Recording Systems. *Appl. Sci.* **2021**, *11*, 4387. [CrossRef]

21.　Nguyen, T.A.; Lee, J. Effective Generalized Partial Response Target and Serial Detector for Two-Dimensional Bit-Patterned Media Recording Channel Including Track Mis-Registration. *Appl. Sci.* **2020**, *10*, 5738. [CrossRef]

22.　Nguyen, T.A.; Lee, J. Two-Dimensional Interference Estimator with Parallel Structure for Holographic Data Storage Channel. *Appl. Sci.* **2022**, *12*, 2112. [CrossRef]

23.　Kim, K.; Kim, S.H.; Koo, G.; Seo, M.S.; Kim, S.W. Decision feedback equalizer for holographic data storage. *Appl. Opt.* **2018**, *57*, 4056–4066. [CrossRef] [PubMed]

24.　Koo, K.; Kim, S.V.; Jeong, J.J.; Kim, S.W. Two-dimensional soft output viterbi algorithm with a variable reliability factor for holographic data storage. *Jpn. J. Appl. Phys.* **2013**, *52*, 09LE03. [CrossRef]

25.　Koo, K.; Kim, S.-Y.; Jeong, J.J.; Kim, S.W. Data page reconstruction method based on two-dimensional soft output Viterbi algorithm with self reference for holographic data storage. *Opt. Rev.* **2014**, *21*, 591–596. [CrossRef]